Automatica 43(9):1508–1518, 2007

Passivity-based designs for synchronized path-following

Ivar-André F. Ihle[a,b], Murat Arcak[c], Thor I. Fossen[b,d]

[a]*Rolls-Royce Marine AS, Stortingsgt. 14, NO-0161 Oslo, Norway*
[b]*Centre for Ships and Ocean Structures, Norwegian University of Science and Technology, NO-7491 Trondheim, Norway* [c]*Department of Electrical, Computer, and Systems Engineering, Rensselaer Polytechnic Institute Troy, NY 12180, USA* [d]*Department of Engineering Cybernetics, Norwegian University of Science and Technology, NO-7491 Trondheim, Norway*

Abstract

We consider a formation control system where individual systems are controlled by a path-following design and the path variables are to be synchronized. We first show a passivity property for the path-following system, and next, combine this with a passivity-based synchronization algorithm developed in Arcak [2007. Passivity as a design tool for group coordination. *IEEE Transactions on Automatic Control*, in press]. The passivity approach expands the classes of synchronization schemes available to the designer. This generality offers the possibility to optimize controllers to, e.g., improve robustness and performance. Two designs are developed in the proposed passivity framework: the first employs the path error information in the synchronization loop, while the second only uses synchronization errors. A sampled-data design, where the path variables are updated in discrete-time and the path-following controllers are updated in continuous time, is also developed.

Keywords: Passivity; Synchronization; Group coordination; Path following; Sampled-data design

1. Introduction

Recent advances in control techniques for vehicles and communication capabilities have sparked an interest in formation control that has resulted in a number of publications with applications ranging from autonomous underwater vehicles (AUVs) to multiple satellite control (see, e.g., Encarnação & Pascoal, 2001; Kumar, Leonard, & Morse, 2005; Ren, Beard, & Atkins, 2005). Examples of marine cooperative control include autonomous oceanographic sampling networks and under-way replenishment operations between marine surface vessels.

The primary goal in *path-following* problems is to design control laws that force the output of a system to follow a desired *path*. The secondary goal for the system is to obey a dynamic assignment such as time, speed or acceleration along the path (Aguiar, Hespanha, & Kokotović, 2005; Do, Jiang, & Pan, 2002; Hauser & Hindman, 1995; Samson, 1992). In particular the formulation in Skjetne, Fossen, and Kokotović (2004) aims to develop control laws that force a system to follow a prescribed path, parameterized by a path variable θ, and that assign a desired speed to be achieved by $\dot{\theta}$ in the limit as $t \to \infty$. In the classical tracking problem the path variable θ is designed to follow a specific time function, such that the system output tracks a time-dependent signal. In the path-following formulation studied in this paper, the priority is to converge to the path while the desired speed profile is to be achieved by $\dot{\theta}$ in the limit. Among other advantages, the path-following approach offers flexibility to shape the transient behavior of $\dot{\theta}$.

In this paper we exploit this flexibility to synchronize the path variables for a group of path-following systems. In particular, we make use of a passivity-based framework for formation control proposed in Arcak (2007). This framework allows us to obtain a broad class of synchronization schemes for a

general communication topology, and encompasses earlier designs such as Ihle, Skjetne, and Fossen (2004). In this framework, we represent the closed-loop system as the feedback interconnection of a dynamic block for path variable synchronization and another block that incorporates the path-following systems. We design each block to be *passive* (see the definition in (3)) and prove stability of their interconnection by using the Passivity Theorem which states that an interconnection of two passive blocks is passive and, thus, stable in the absence of exogenous inputs.

A major advantage of the passivity approach is that it allows the designer to construct filters that preserve passivity properties of the closed-loop system. This additional flexibility may be used to improve the performance and robustness of the design. We further consider a sampled-data framework where the synchronization scheme is implemented in discrete time while the path-following controllers are continuous-time systems. This formulation is meaningful because communication of path parameters between vehicles will likely occur over a digital network which introduces delays, while the path-following controllers are implemented locally in continuous time or with fast sampling.

The rest of this paper is organized as follows: Section 2 gives an overview of the path-following problem. Section 3 presents two passivation designs for synchronization and gives the main stability results. A sampled-data scheme for synchronization and path-following is given in Section 4. Examples of filter design and simulations that illustrate synchronization properties are presented in Section 5. Concluding remarks are given in Section 6.

1.1. Preliminaries

The notation in this paper is as follows. For a matrix $P = P^\top > 0$, we let $\lambda_{\min}(P)$ and $\lambda_{\max}(P)$ be the minimum and maximum eigenvalue of P, respectively. In abbreviations like GS, GAS, UGES, etc., U stands for uniform, G for global, A for asymptotic, E for exponential, and S for stable.

A *parameterized path* is a geometric curve

$$Y_d := \{y \in \mathbb{R}^m : \exists \theta \in \mathbb{R} \text{ such that } y = y_d(\theta)\},$$

where y_d is continuously parameterized by the path variable θ (Skjetne et al., 2004). We will also sometimes call y_d as the path.

A function $\alpha : \mathbb{R}_{\geqslant 0} \to \mathbb{R}_{\geqslant 0}$ is of class $\mathcal{K}$ if it is continuous, strictly increasing and satisfies $\alpha(0) = 0$. A function $\beta : \mathbb{R}_{\geqslant 0} \times \mathbb{R}_{\geqslant 0} \to \mathbb{R}_{\geqslant 0}$ is of class $\mathcal{KL}$ if, for each fixed s, the function $\beta(r, s)$ belongs to class $\mathcal{K}$ with respect to r and, for each fixed r, the function $\beta(r, s)$ is decreasing with respect to s and $\beta(r, s) \to 0$ as $s \to \infty$.

The system $\dot{x} = f(x, u)$ is said to be input-to-state stable (ISS) if there exist functions $\beta \in \mathcal{KL}$, $\rho \in \mathcal{K}$ such that for any initial state $x(t_0)$ and any bounded input $u(t)$, the solution $x(t)$ exists for all $t \geqslant 0$ and satisfies

$$|x(t)| \leqslant \beta(|x(t_0)|, t - t_0) + \rho\left(\sup_{t_0 \leqslant \tau \leqslant t} |u(\tau)|\right). \tag{1}$$

The dynamic system

$$\begin{aligned} \dot{x} &= f(x, u), \\ y &= h(x, u), \quad x \in \mathbb{R}^n, \ \ u, y \in \mathbb{R}^p \end{aligned} \tag{2}$$

is said to be *passive* if there exists a continuously differentiable storage function $V(x) \geqslant 0$ such that

$$\dot{V} \leqslant -W(x) + u^\top y \tag{3}$$

for some positive semi-definite function $W(x)$. We say that (2) is *strictly* passive if $W(x)$ is positive definite. A static nonlinearity $y = h(u)$ is passive if, for all $u \in R^m$,

$$u^\top y = u^\top h(u) \geqslant 0; \tag{4}$$

and strictly passive if (4) holds with strict inequality $\forall u \neq 0$.

2. Problem formulation

Consider a system

$$\begin{aligned} \dot{x} &= f(x, u), \\ y &= h(x), \end{aligned} \tag{5}$$

where $x \in \mathbb{R}^n$ denotes the state vector, $y \in \mathbb{R}^m$ is the system output, and $u \in \mathbb{R}^n$ is the control. To force y to a prescribed feasible path $y_d(\theta)$, and to assign a feasible speed $\upsilon(t)$ to $\dot{\theta}$ on this path, Skjetne et al. (2004) studies subclasses of (5) and develops maneuvering design procedures based on feedback linearization and backstepping techniques. Other techniques for path following are considered in, e.g., Aguiar et al. (2005), Al-Hiddabi and McClamroch (2002), Do et al. (2002), Encarnação and Pascoal (2001), and Hauser and Hindman (1995). The designs in Skjetne et al. (2004) lead to a closed-loop system of the form

$$\begin{aligned} \dot{z} &= F(x)z - g(t, x, \theta)\omega, \\ \dot{\theta} &= \upsilon(t) - \omega, \end{aligned} \tag{6}$$

where z is a set of new variables that include the path-following error $y - y_d(\theta)$ and its derivatives, and ω is a feedback term to be designed such that the desired speed $\upsilon(t)$ is recovered asymptotically; that is

$$\omega \to 0 \quad \text{as } t \to \infty. \tag{7}$$

$F(x) \in \mathbb{R}^{n \times n}$ and $g(t, x, \theta) \in \mathbb{R}^n$ depend on the control design and, in particular, $F(x)$ satisfies

$$PF(x) + F(x)^\top P \leqslant -I \tag{8}$$

for some matrix $P = P^\top > 0$. A path-following design for marine vehicles is presented in Section 5.

Assumption 1. We assume that the function $g(t, x, \theta)$ is uniformly bounded in its arguments—see Skjetne et al. (2004, Assumption 2.1)

In this paper, we consider a group of vehicles $i = 1, \ldots, r$, each controlled by an individual path-following design with a

prescribed velocity $\upsilon(t)$ assigned to the group, resulting in the closed-loop system

$$\dot{z}_i = F_i(x_i)z_i - g_i(t, x_i, \theta_i)\omega_i,$$
$$\dot{\theta}_i = \upsilon(t) - \omega_i. \tag{9}$$

In this paper we assume that the speed assignment $\upsilon(t)$ is identical for all vehicles, and is independent of the path variable θ_i. This assumption does not pose a severe restriction on the choice of paths as our example in Section 5 illustrate. However, a θ_i-dependent speed assignment may be desirable for more complicated paths, and will be investigated in future work.

Our goal is to design ω_i to synchronize the path variables θ_i, $i = 1, \ldots, r$, while achieving (7). All path parameters are collected in the vector $\theta = [\theta_1, \ldots, \theta_r]^\top$. The design of ω_i depends on variables of the ith system and on the path parameters for the neighboring vehicles, so only one scalar variable needs to be transmitted from each vehicle. The communication topology between the members of the formation is described by a graph $\mathcal{G}$. Two members, i and j, are *neighbors* if they can access the synchronization error $\theta_i - \theta_j$. In this case, we let the ith and jth vertices of $\mathcal{G}$ be connected by an edge. The information flow is bidirectional, but to simplify the derivation we assign an orientation to the graph by considering one of the vertices to be the positive end of the edge. For a group of r members with p edges, the $r \times p$ incidence matrix $D(\mathcal{G})$ is defined, for the edge k (Godsil & Royle, 2001):

$$d_{ik} = \begin{cases} +1 & \text{if } i\text{th vertex is the positive end of } k, \\ -1 & \text{if } i\text{th vertex is the negative end of } k, \\ 0 & \text{otherwise.} \end{cases} \tag{10}$$

Assumption 2. We assume that $\mathcal{G}$ is a connected graph, i.e. a path exists between every two distinct vertices of $\mathcal{G}$.

3. Passivation designs for synchronization

3.1. Design 1: with path error feedback

When the path error is available for feedback we design $\omega = [\omega_1, \ldots, \omega_r]^\top$ as

$$\omega_i = \mathcal{F}_i\{2z_i^\top P_i g_i + \psi_i(\theta)\}, \tag{11}$$

where $\mathcal{F}_i\{\cdot\}$ denotes the output of a static or dynamic block, which will be specified. This $\mathcal{F}_i$ can be a filter added to enhance performance and robustness properties, as illustrated with examples in Section 5. The input to this filter is

$$u_i := 2z_i^\top P_i g_i + \psi_i(\theta), \tag{12}$$

where the first component is the path error feedback $2z_i^\top P_i g_i$, which serves to improve convergence properties to the desired path (Skjetne, Teel, & Kokotović, 2002). The second component ψ_i is for the synchronization of the path parameters, and is designed as

$$\psi_i(\theta) = \sum_{k=1}^{p} d_{ik}\phi_k(\theta_i - \theta_k), \tag{13}$$

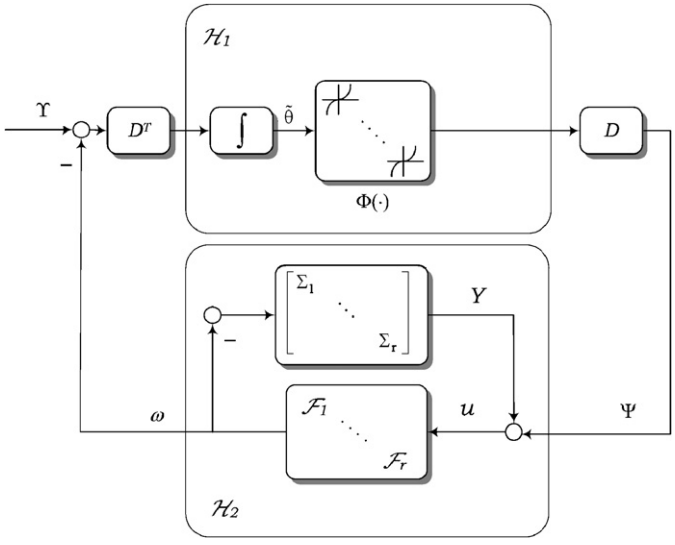

Fig. 1. Block diagram for the synchronized path-following control system. Υ is an $r \times 1$ vector with each entry equal to $\upsilon(t)$.

where ϕ_k is a sector nonlinearity, that is

$$x\phi_k(x) > 0 \ \ \forall x \neq 0 \quad \text{and} \quad \lim_{|x|\to\infty} \int_0^x \phi_k(\sigma)\, \mathrm{d}\sigma = +\infty. \tag{14}$$

The feedback law (11) is implementable with local information because it depends only on the neighbors of the ith member ($d_{ik} \neq 0$). With ω as in (11), the total closed-loop system can be represented as in Fig. 1, where Σ_i is the z_i-subsystem as in (9),

$$\tilde{\theta} := D^\top\theta, \quad \mathcal{F} := \mathrm{diag}(\mathcal{F}_1, \ldots, \mathcal{F}_r),$$
$$\Phi(\cdot) = [\phi_1(\cdot), \ldots, \phi_p(\cdot)]^\top, \quad \Psi(\theta) = [\psi_1, \ldots, \psi_r]^\top \tag{15}$$

and

$$Y := 2z^\top PG, \quad u = Y + \Psi, \tag{16}$$

where $z := [z_1^\top, \ldots, z_r^\top]^\top$, $P := \mathrm{diag}(P_1, \ldots, P_r)$, for $P_i = P_i^\top > 0$, and $G := \mathrm{diag}(g_1, \ldots, g_r)$. In particular, note from (10) that $\tilde{\theta}$ in (15) is a vector that consists of the differences between the path parameters of neighboring vehicles. Because the graph $\mathcal{G}$ is connected, $\tilde{\theta} = 0$ is achieved if and only if all path parameters are synchronized.

We investigate stability properties of the closed loop by separating it into two blocks, $\mathcal{H}_1$ and $\mathcal{H}_2$, as in Fig. 1, and analyze passivity properties of each block. The Passivity Theorem guarantees that the negative feedback interconnection of two passive systems is passive and, thus, stable in the absence of exogenous inputs (Khalil, 2002). Although Υ, which is an $r \times 1$ vector with each entry equal to $\upsilon(t)$, appears as an exogenous input in Fig. 1, it lies in the null space of the proceeding block D^T because its entries are identical. Following Arcak (2007) we now characterize the properties that $\mathcal{F}_i$'s must possess to ensure passivity of $\mathcal{H}_2$ and appropriate detectability conditions that are used to guarantee asymptotic convergence. If $\mathcal{F}_i$ is a

static block we restrict it to be of the form

$$\omega_i = h_i(u_i), \tag{17}$$

where $h_i : \mathbb{R} \to \mathbb{R}$ is a locally Lipschitz function satisfying the sector property

$$u_i h_i(u_i) > 0 \quad \forall u_i \neq 0. \tag{18}$$

If $\mathscr{F}_i$ is a dynamic block of the form

$$\begin{aligned} \dot{\xi}_i &= f_i(\xi_i) + g_i(\xi_i)u_i, \quad \xi_i \in \mathbb{R}^{n_i}, \\ \omega_i &= h_i(\xi_i) + j_i(\xi_i)u_i \end{aligned} \tag{19}$$

we assume $f_i(\cdot), g_i(\cdot), h_i(\cdot)$ and $j_i(\cdot)$ are locally Lipschitz functions such that $f_i(0) = 0$ and $h_i(0) = 0$. Our main restriction on (19) is that it be passive with a twice continuously differentiable, positive definite, radially unbounded storage function $S_i(\xi_i)$ satisfying

$$\dot{S}_i \leqslant -W_i(\xi_i) + u_i\omega_i - v_i u_i^2, \quad v_i \geqslant 0 \tag{20}$$

for some positive definite function $W_i(\xi_i)$. Inequality (20) with $v_i > 0$ is an *input-strict passivity* property which is possible only when the relative degree of (19) is zero. Our asymptotic stability proof below allows $v_i = 0$ provided that (19) have a well defined relative-degree-one at $\xi_i = 0$. According to Sepulchre, Janković, and Kokotović (1997, Proposition 2.44), this is indeed the case if

$$j_i(\xi_i) \equiv 0, \quad g_i(0) \neq 0, \quad \left.\frac{\partial h_i(\xi_i)}{\partial \xi_i}\right|_{\xi_i=0} \neq 0. \tag{21}$$

We thus make the following assumption:

Assumption 3. If $v_i = 0$ in (20) then (21) holds.

With $\mathscr{H}_1$ and $\mathscr{H}_2$ designed as above, we prove UGAS for $(\tilde{\theta}, z, \xi) = 0$ in Theorem 1. This UGAS property implies that in the limit as $t \to \infty$ the path parameters θ are synchronized ($\tilde{\theta} \to 0$) and that each system i follows its desired path ($z_i \to 0$). Furthermore $\omega \to 0$ which means that $\dot{\theta}$ in (6) recovers the speed assignment $\upsilon(t)$.

Theorem 1. *Consider the feedback interconnection shown in Fig. 1 where members $i = 1, \ldots, r$ are interconnected in a formation as described by* (10), *$\phi_k, k = 1, \ldots, p$ is as in* (14), *and $\mathscr{F}_i, i = 1, \ldots, r$ are designed as in* (17)–(20). *Under Assumptions* 1–3 *the feedforward path $\mathscr{H}_1$ is passive from $\dot{\tilde{\theta}}$ to Φ, and the feedback path $\mathscr{H}_2$ is strictly passive from Ψ to ω. Furthermore the origin of the feedback interconnection $(\tilde{\theta}, z, \xi) = 0$ is UGAS.*

Proof. We combine ideas from Ihle et al. (2004), Arcak (2007), and specific results for path following from Skjetne et al. (2004). To prove passivity from $\dot{\tilde{\theta}}$ to Φ, let

$$V_\psi := \sum_{k=1}^{p} \int_0^{\tilde{\theta}_k} \phi_k(\sigma)\, \mathrm{d}\sigma. \tag{22}$$

Since ϕ_k is as in (14), V_ψ is a positive definite, radially unbounded storage function for $\mathscr{H}_1$. Differentiating (22) with respect to time yields

$$\dot{V}_\psi = \sum_{i=1}^{p} \phi_i(\theta_i - \theta_{i+1}) \cdot (\dot{\theta}_i - \dot{\theta}_{i+1}) = \Phi^\top \cdot \dot{\tilde{\theta}}, \tag{23}$$

which proves that the mapping from $\dot{\tilde{\theta}}$ to Φ is indeed passive. It follows that the path from $-\omega$ to Ψ is also passive. To see this substitute $\dot{\tilde{\theta}} = D\,(\Upsilon - \omega)$ in (23) and note that the sum of the rows of D being zero and the entries of Υ being equal imply $D\Upsilon = 0$. Thus,

$$\dot{V}_\psi = -\Phi^\top D^\top \omega = -\Psi^\top \omega. \tag{24}$$

To prove passivity of the feedback path, we first consider the Σ_i-blocks. The storage function

$$V_z = \sum_{i=1}^{r} z_i^\top P_i z_i, \tag{25}$$

where P_i is as in (8) yields the following time-derivative along the trajectories of z

$$\dot{V}_z \leqslant -\sum_{i=1}^{r} z_i^\top z_i - Y^\top \omega \tag{26}$$

which proves that the Σ-block is strictly passive from $-\omega$ to Y. To establish passivity of $\mathscr{F}$, we let $\mathscr{I}$ denote the subset of indices $i = 1, \ldots, r$ for which $\mathscr{F}_i$ is a dynamic block as in (19), and employ the storage function

$$V_f := \sum_{i \in \mathscr{I}} S_i(\xi_i) \tag{27}$$

which yields

$$\dot{V}_f = \sum_{i \in \mathscr{I}} \dot{S}_i \leqslant \sum_{i \in \mathscr{I}} (-W_i(\xi_i) + u_i\omega_i - v_i u_i^2) \tag{28}$$

$$\leqslant \sum_{i \in \mathscr{I}} (-W_i(\xi_i) - v_i u_i^2) + u^\top \omega - \sum_{i \notin \mathscr{I}} u_i \omega_i. \tag{29}$$

Substitution of $u = Y + \Psi$ then yields

$$\dot{V}_f \leqslant \sum_{i \in \mathscr{I}} (-W_i(\xi_i) - v_i u_i^2) + Y^\top \omega + \Psi^\top \omega - \sum_{i \notin \mathscr{I}} u_i \omega_i. \tag{30}$$

To conclude passivity of the feedback path we use the storage function

$$V_{fb}(z, \xi) := V_z(z) + V_f(\xi) \tag{31}$$

and, obtain by adding (26) and (30),

$$\dot{V}_{fb} \leqslant \sum_{i \in \mathscr{I}} (-W_i(\xi_i) - v_i u_i^2) - \sum_{i=1}^{r} z_i^\top z_i + \Psi^\top \omega - \sum_{i \notin \mathscr{I}} u_i \omega_i. \tag{32}$$

Finally, since the static blocks satisfy (18),

$$\sum_{i\notin\mathscr{I}} u_i\omega_i = \sum_{i\notin\mathscr{I}} u_i h_i(u_i) \geqslant 0. \tag{33}$$

We thus obtain

$$\dot{V}_{fb} \leqslant -\sum_{i\in\mathscr{I}} W_i(\xi_i) - \sum_{i=1}^{r} z_i^\top z_i + \Psi^\top\omega \tag{34}$$

and conclude that the feedback path is strictly passive from Ψ to ω.

To prove stability of $(\tilde{\theta}, z, \xi) = 0$ we use the Lyapunov function

$$V(\tilde{\theta}, z, \xi) = V_\psi(\tilde{\theta}) + V_{fb}(z, \xi) \tag{35}$$

which from (24) and (32), gives the time-derivative:

$$\dot{V} \leqslant -\sum_{i\in\mathscr{I}} W_i(\xi_i) - \sum_{i=1}^{r} z_i^\top z_i - \sum_{i\notin\mathscr{I}} u_i h_i(u_i) - \sum_{i\in\mathscr{I}} v_i u_i^2. \tag{36}$$

Since the right-hand side is negative semi-definite we conclude that the trajectories $(z(t), \xi(t), \tilde{\theta}(t))$ are uniformly bounded on the interval $t \in [t_0, t_0 + T]$, for any T within the maximal interval of existence. Due to the boundedness of the speed assignment $v(t)$, it follows that $(\theta(t), x(t))$ is bounded by a continuous function of T and, thus, there are no finite escape times. This implies that $\tilde{\theta}(t)$ and $z(t)$ are well defined for all $t \geqslant t_0$ and, from (36), the equilibrium $(z, \xi, \tilde{\theta}) = 0$ is uniformly stable.

To prove uniform asymptotic stability we use the Nested Matrosov Theorem (Loría, Panteley, Popović, & Teel, 2005). To this end we define the auxiliary function

$$V_2 = -\tilde{\theta}^\top D^+ \Lambda\omega, \tag{37}$$

where D^+ denotes the pseudo-inverse of the incidence matrix D, and Λ is a diagonal matrix with entries

$$\Lambda_{ii} = \begin{cases} (L_{g_i} h_i(0))^{-1} & \text{if } i \in \mathscr{I} \text{ and } v_i = 0, \\ 0 & \text{if } i \notin \mathscr{I} \text{ or } v_i > 0. \end{cases} \tag{38}$$

In particular $L_{g_i} h_i(0) := \partial h_i(\xi_i)/\partial\xi_i|_{\xi_i=0} g_i(0)$ is nonsingular and, thus, invertible because of the passivity of the ξ_i-subsystems and because of assumption (21) (Sepulchre et al., 1997, Proposition 2.44). To apply Matrosov's Theorem we denote by Y_1 the right-hand side of (36) and claim that

$$Y_1 = 0 \;\Rightarrow\; \dot{V}_2 =: Y_2 \leqslant 0. \tag{39}$$

To see this note that $Y_1 = 0$ implies $\xi = 0$ and $\omega = 0$, which mean that all terms in $\dot{V}_2$ vanish except

$$-\tilde{\theta}^\top D^+ \Lambda\dot{\omega}|_{Y_1=0}. \tag{40}$$

Because $\dot{\omega}_i|_{\xi=0} = L_{g_i} h_i(0) u_i$ when $i \in \mathscr{I}$ and $v_i = 0$, and because $Y_1 = 0$ implies $u_i = 0$ when $i \notin \mathscr{I}$ or $v_i > 0$, we conclude from (38) that $\Lambda\dot{\omega}|_{Y_1=0} = u$ and rewrite (40) as

$$-\tilde{\theta}^\top D^+ u. \tag{41}$$

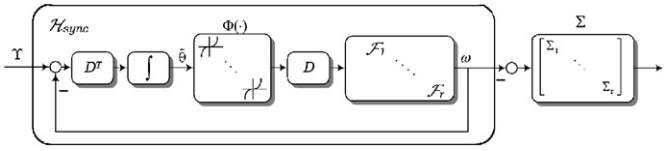

Fig. 2. Cascade interconnection for Design 2.

We then substitute $\tilde{\theta} = D^\top\theta$ in (41), and using the property $DD^+D = D$ of the pseudo-inverse, and noting that $Y_1 = 0$ means $z = 0$ which in turn implies $u = \Psi = D\Phi(\tilde{\theta})$, we conclude

$$Y_1 = 0 \Rightarrow Y_2 = -\theta^{\mathrm{T}} DD^+ D\Phi(\tilde{\theta}) = -\theta^{\mathrm{T}} D\Phi(\tilde{\theta}) = -\tilde{\theta}^{\mathrm{T}}\Phi(\tilde{\theta}). \tag{42}$$

Because $\tilde{\theta}^\top\Phi(\tilde{\theta})$ is positive definite in $\tilde{\theta}$ from (14), Eq. (42) proves the claim (39). It further follows from (36) and (42) that $Y_1 = 0$ and $Y_2 = 0$ together imply $(z, \xi, \tilde{\theta}) = 0$. All assumptions of Loría et al. (2005, Theorem 1) being satisfied we conclude UGAS of $(z, \xi, \tilde{\theta}) = 0$. □

Remark 2. A special case of (11), studied in Ihle et al. (2004), is when the neighbors for system i are system $i-1$ and system $i+1$, i.e., the synchronization error is $\tilde{\theta} = [\theta_1 - \theta_2, \ldots, \theta_{r-1} - \theta_r]^\top$. Ihle et al. (2004) further assumes that $\mathscr{F}$ is a constant gain matrix and $\phi_i(r) = r^{2p-1}$, for $p = 1, 2, 3, \ldots$. In contrast, in this paper we have considered a general communication topology, and derived relaxed conditions on the feedback block and synchronization function. In particular, $\mathscr{F}_i$'s are not necessarily constant gains and ϕ_i's are not necessarily polynomials.

3.2. Design 2: without path error feedback

We next consider a design where ω_i only depends on the synchronization terms, and not on the path error. The update law for ω_i is now

$$\omega_i = \mathscr{F}_i\{\psi_i(\theta)\}, \tag{43}$$

where $\mathscr{F}_i$ and ψ_i are as in Section 3.1. Without the path error feedback, the closed-loop system becomes a cascade of $\mathscr{H}_{\text{sync}}$ and Σ as in Fig. 2. The origin of $\mathscr{H}_{\text{sync}}$, $(\tilde{\theta}, \xi) = 0$, is proved to be GAS in Arcak (2007) which means that $\omega \to 0$. In Theorem 3 we prove that the Σ-block is ISS (Sontag, 1989) w.r.t. ω. Stability of the closed-loop system then follows because a cascade of an ISS and a UGAS system is UGAS (Sontag, 1989; Sontag & Teel, 1995).

Theorem 3. *Consider the cascaded system in Fig. 2, where members $i = 1, \ldots, r$ are interconnected in a formation as described by* (10)*, $\phi_k, k = 1, \ldots, p$ are as in* (14)*, and $\mathscr{F}_i, i = 1, \ldots, r$ are designed as in* (17)–(20)*. Then, the origin of $\mathscr{H}_{\text{sync}}$-block is GAS, the Σ block is ISS with respect to ω, and the origin $(\tilde{\theta}, \xi, z) = 0$ is UGAS.*

Proof. For completeness, the stability proof for $\mathscr{H}_{\text{sync}}$ is given here: the feedforward path of the $\mathscr{H}_{\text{sync}}$-block is an interconnection of a passive and a strictly passive block. Since

pre- and post-multiplication of a matrix and its transpose does not change passivity properties the forward path is passive and with negative feedback the block is output strictly passive from v to ω. Moreover, when $\Upsilon = 0$, due to (21):

$$\omega \equiv 0 \;\Rightarrow\; \mathscr{F}\{D\Phi(\tilde{\theta})\} \equiv 0 \;\Rightarrow\; D\Phi(\tilde{\theta}) \equiv 0 \tag{44}$$

which implies that $\Phi(\tilde{\theta})$ lies in the nullspace $\mathscr{N}(D)$. When D has linearly independent columns $\mathscr{N}(D)=0$ and hence $\Phi(\tilde{\theta}) \equiv 0 \;\Rightarrow\; \tilde{\theta} \equiv 0$ due to (14). When D has linearly dependent columns, the null space of D is nontrivial. However, a simultaneous solution to $\Phi(\tilde{\theta}) \in \mathscr{N}(D)$ and $\tilde{\theta} \in \mathscr{R}(D^\top)$ is possible only when $\tilde{\theta} = 0$. This is because $\mathscr{R}(D^\top)$ and $\mathscr{N}(D)$ are orthogonal to each other, which means $\tilde{\theta}^\top \Phi(\tilde{\theta}) = 0$, and we conclude from (14) that $\tilde{\theta}=0$. Hence, the $\mathscr{H}_{\text{sync}}$-block is zero-state observable (Khalil, 2002). From Khalil (2002, Lemma 6.7) we obtain GAS of the origin $\tilde{\theta} = 0$.

To prove the ISS-property we rewrite the time-derivative (26) as

$$\begin{aligned}\dot{V}_z &\leqslant \sum_{i=1}^{r}(-z_i^\top z_i - 2z_i^\top P_i g_i \omega_i)\\ &\leqslant \sum_{i=1}^{r}(-|z_i|^2 + 2p_{iM}\delta_{gi}|z_i||\omega_i|),\end{aligned}$$

where δ_{gi} is an upper bound on g_i due to Assumption 1. Furthermore, we get

$$|z_i| \geqslant \frac{2p_{iM}\delta_{gi}|\omega_i|}{\varepsilon} \;\Rightarrow\; \dot{V}_z \leqslant \sum_{i=1}^{r}(-(1-\varepsilon)|z_i|^2), \tag{45}$$

where $0 < \varepsilon < 1$. Thus, the system is ISS (Khalil, 2002) from ω_i to z_i with $\rho(r) = (2p_{iM}\delta_{gi}/\varepsilon)r$. Since the origin of $\mathscr{H}_{\text{sync}}$ is GAS and Σ is ISS with respect to ω, it follows from Sontag and Teel (1995) that the origin $(\tilde{\theta}, \xi, z) = 0$ is UGAS. □

Remark 4. Using the results on agreement protocols in Arcak (2007), the results can be extended to a time-varying communication topology given by the incidence matrix $D(t)$ as long as $\mathscr{G}$ remains connected for all $t > 0$. A further result in Arcak (2007) allows the graph to lose connectivity pointwise in time as long as it is established in an integral sense. This means that signal dropouts in the communication links can be tolerated if connectivity is eventually re-established.

4. Sampled-data design with discrete-time update for θ

We now study the situation where the path parameters θ_i are updated in discrete time. Such an implementation is practically relevant, because path parameters are to be exchanged over a communication network where the transmission occurs at discrete-time intervals. Since the path-following controllers can be implemented locally by each vehicle with fast sampling, we consider the Σ-blocks in Fig. 1 to be continuous time. This implementation thus results in the sampled-data closed-loop system:

$$\begin{aligned}\dot{z}_i &= F_i(x_i)z_i - g_i(t, x_i, \theta^{\text{zoh}})\omega_i^{\text{zoh}},\\ \theta_i((n+1)T) &= \theta_i(nT) + \upsilon(nT) - \omega_i(nT),\end{aligned} \tag{46}$$

where $n = 0, 1, 2, \ldots$ is the time index, and ω_i^{zoh} and θ^{zoh} denote the zero-order-hold equivalent continuous-time signals generated from the discrete-time signals θ_i and ω_i. Because θ is now updated in discrete time the integral block in the feedforward path of Fig. 1 is replaced by a summation block, and $\dot{\tilde{\theta}}$ is replaced by

$$\delta\tilde{\theta} := \tilde{\theta}((n+1)T) - \tilde{\theta}(nT). \tag{47}$$

As discussed in Arcak (2007), passivity of the feedforward path $\mathscr{H}_1$ cannot be achieved in discrete time because the phase lag of a summation block exceeds 90°. In the feedforward system we restrict the slope of the nonlinearity $\phi_k(\tilde{\theta}_k)$ by

$$\phi_k'(\tilde{\theta}_k) \leqslant \mu \tag{48}$$

for some constant $\mu > 0$. With this assumption it is shown in Arcak (2007) that the storage function $V_\psi(\theta)$ in (22) satisfies

$$V_\psi(\tilde{\theta}((n+1)T)) - V_\psi(\tilde{\theta}(nT)) \leqslant -\Psi^\top\omega + \frac{\mu\lambda_N}{2}\omega^\top\omega, \tag{49}$$

where λ_N denotes the largest eigenvalue of the graph Laplacian matrix $DD^\top$ and the second term on the right-hand side of (49) quantifies the shortage of passivity. Then, the $\mathscr{H}_2$-block must achieve an excess of passivity in the feedback path to guarantee stability for the interconnected system.

4.1. Design 1: with path error feedback

When $z(t)$ is available for feedback we design ω_i in (46) as

$$\begin{aligned}\omega_i(nT) = \gamma_i(&2z_i(nT)^\top P_i g_i(nT, x_i(nT), \theta(nT))\\ &+ \psi_i(\theta(nT))),\end{aligned} \tag{50}$$

where $\gamma_i > 0$ is an adaptation gain to be specified and $\psi_i(\cdot)$ is as in (13). With this design the $\mathscr{H}_2$ block is as in Fig. 3 and, as we shall see, its excess of passivity compensates for the shortage in (49) when γ_i and T are sufficiently small. To make this claim precise we need the following lemma, proven in Biyik and Arcak (2006, Chapter 2) using the techniques of Laila, Nešić, and Teel (2002):

Lemma 5 (*Biyik & Arcak, 2006, Chapter 2*). *Consider members $i = 1, \ldots, r$ interconnected as described by the graph representation* (10), *and let $\tilde{\theta}_k$, $k = 1, 2, \ldots, p$ denote the differences between the variables θ_i of neighboring members. Let $\phi_k(\tilde{\theta}_k)$'s be designed as a first-third quadrant nonlinearity satisfying* (48) *for some constant $\mu > 0$. Suppose that $\mathscr{H}_i$'s are sampled-data dynamic blocks as in Fig. 3, and satisfy the following two assumptions*:

L1. *For $\omega_i = 0$, the time-derivative of V_{zi} for Σ_i is upper bounded by $\dot{V}_{zi}(z_i) \leqslant -C|z_i|^2$ for some $C > 0$,*

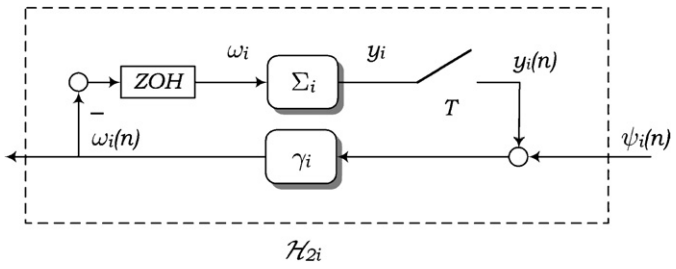

Fig. 3. A block diagram representation of the sampled-data dynamical block $\mathscr{H}_{2i}$ where *ZOH* stands for the "zero-order-hold" function and T is the sampling period.

L2. *Σ_i-subsystems, $i = 1, \ldots, r$ are ISS from ω_i to y_i, i.e., there exist class-$\mathscr{KL}$ and class-$\mathscr{K}$ functions $\beta(\cdot,\cdot)$ and $\rho(\cdot)$, respectively, such that*

$$|z_i(t)| \leqslant \beta(|z_i(t_0)|, t - t_0) + \rho\left(\sup_{t_0 \leqslant \tau \leqslant t} |\omega_i(\tau)|\right).$$

Then given compact sets $\mathscr{D}_{\tilde{\theta}}$ and $\mathscr{D}_z$ there exist positive constants $\bar{T}$ and $\bar{\gamma}$ such that for all sampling periods $T < \bar{T}$ and $\gamma_i \leqslant \bar{\gamma}$, the feedback law (50) *achieves asymptotic stability of the origin $(\tilde{\theta}, z) = 0$ with a region of attraction that includes $\mathscr{D}_{\tilde{\theta}} \times \mathscr{D}_z$.*

Lemma 5 proves a semi-global asymptotic stability property in T and γ_i for the equilibrium $(\tilde{\theta}, z) = 0$, which means that any prescribed region of attraction can be achieved by sufficiently reducing the sampling period T and the adaptation gain γ_i. In particular, increasing the size of the prescribed region of attraction or increasing the parameters μ and λ_N in (49) dictate smaller values for $\bar{T}$ and $\bar{\gamma}$ (see Biyik & Arcak, 2006, Chapter 2 for formulas that estimate $\bar{T}$ and $\bar{\gamma}$). The proof in Biyik and Arcak (2006, Chapter 2) (see also Laila et al., 2002) is also applicable to time-varying sampling periods that are upper-bounded by $\bar{T}$. We now apply Lemma 5 to our system and state the main result of this section:

Theorem 6. *Consider members $i = 1, \ldots, r$ interconnected in a formation as described by* (10). *Let ϕ_k's be as in* (14) *and* (48), *and suppose that $\mathscr{H}_2$ consists of sampled-data dynamic blocks as in Fig. 3 where the continuous-time Σ_i-block and the discrete-time updates for θ_i are as given in* (46). *Then, given compact sets $\mathscr{D}_z$ and $\mathscr{D}_\theta$ there exist positive constants $\bar{T}$ and $\bar{\gamma}$ such that for all sampling periods $T < \bar{T}$ and $\gamma_i \leqslant \bar{\gamma}$, the feedback law* (50) *achieves asymptotic stability of the origin $(z, \tilde{\theta}) = 0$ with a region of attraction that includes $\mathscr{D}_z \times \mathscr{D}_{\tilde{\theta}}$.*

Proof. First, we know from the proof of Theorem 1 that each Σ_i-block is strictly passive with a positive definite storage function $V_{z_i}(z_i)$ such that $\dot{V}_{z_i} \leqslant -W(z_i) - y_i\omega_i$ where $W(z_i) = z_i^\top z_i$. Hence, we find a lower bound on $W(z_i) \geqslant C|z_i|^2$ where $C = 1 > 0$ so L1 of Lemma 5 holds. Second, L2 holds since Input-to-State Stability from ω_i to z_i is proved in Theorem 3 using the same storage function. We thus conclude that the origin $(z, \tilde{\theta}) = 0$ is asymptotically stable with a region of attraction that includes the prescribed set $\mathscr{D}_z \times \mathscr{D}_{\tilde{\theta}}$. □

4.2. Design 2: without path error feedback

We next consider the case where $z_i(t)$ is not employed in discrete-time θ_i updates. In this case we have

$$\omega_i(nT) = \mathscr{F}_i\{\psi_i(\theta(nT))\}, \tag{51}$$

where $\mathscr{F}_i$ is a discrete-time dynamic or static block. In order to guarantee excess of passivity in the feedback path, we restrict static $\mathscr{F}_i$ blocks $y_i = h_i(t, u_i)$ by

$$u_i y_i - \tau_i y_i^2 \geqslant \varpi_i(u_i), \tag{52}$$

where $\varpi_i(u_i)$ is a positive definite function and $\tau_i > 0$ quantifies the excess of passivity. When $\mathscr{F}_i$ is a dynamic block of the form

$$\begin{aligned} &\xi_i((n+1)T) = f_i(\xi_i(nT), u_i(nT)), \quad \xi_i \in \mathbb{R}^{n_i}, \\ &y_i = h_i(\xi_i, u_i) \end{aligned} \tag{53}$$

we assume that (21) holds and that there exists a positive definite and radially unbounded storage function $S_i(\xi_i)$ satisfying

$$S_i(\xi((n+1)T)) - S_i(\xi_i(nT)) \leqslant -W_i(\xi_i) + u_i y_i - \tau_i y_i^2 \tag{54}$$

for some positive definite function $W_i(\cdot)$. We then guarantee stability of the feedback system by choosing

$$\tau_i \geqslant \frac{\mu\lambda_N}{2}, \quad i = 1, \ldots, r. \tag{55}$$

As before, GAS of $\tilde{\theta} = 0$ implies $\omega \to 0$ and stability of the path errors follows from the cascade structure and the ISS-property of the Σ_i-subsystems driven by ω:

Theorem 7. *Consider members $i = 1, \ldots, r$ interconnected in a formation as described by* (10). *Let $\phi_k, k = 1, \ldots, p$ be as in* (14) *and* (48), *and suppose that $\mathscr{H}_2$ consists of sampled-data dynamic blocks where the continuous-time Σ_i-blocks are as given in* (9) *and $\mathscr{F}_i$'s are as in* (52)–(54). *Under these conditions if* (55) *holds then the update law* (51) *renders the origin $(\tilde{\theta}, \xi, z) = 0$ GAS.*

Proof. When (55) holds asymptotic stability of $(\tilde{\theta}, \xi) = 0$ follows from Arcak (2007). Furthermore, from Theorem 3 we know that each z_i is ISS with respect to ω_i so $z(t)$ is bounded within each sampling period and constant between the sampling points. It then follows from arguments similar to those in Theorem 3 that the origin $(\tilde{\theta}, \xi, z) = 0$ is GAS. □

5. Examples

We now study a formation maneuvering operation between marine surface vessels to illustrate the proposed framework. The passivity framework is applied to obtain an extended class

of feedback functions $\mathscr{F}_i$ that can address performance properties, increase robustness to thruster saturation, and communication delays for a group of vessels.

We consider a model of a fully actuated tugboat in three degrees of freedom where the surge mode is decoupled from the sway and yaw mode due to port/starboard symmetry. The body-fixed equations of motion for vessel $i=1,\ldots,r$ are given as (see Fossen, 2002 for details)

$$\dot{\eta}_i = R(\psi_i)v_i, \tag{56a}$$

$$M_i\dot{v}_i + C_i(v_i)v_i + D_i(v_i)v_i = \tau_i, \tag{56b}$$

where $\eta_i = [x_i, y_i, \psi_i]^\top$ is the earth-fixed position vector, (x_i, y_i) is the position on the ocean surface and ψ_i is the heading angle (yaw), and $v_i = [u_i, v_i, r_i]^\top$ is the body-fixed velocity vector. The model matrices M_i, C_i, and D_i denote inertia, Coriolis plus centrifugal, and damping, respectively. The numerical values are taken from Ihle, Jouffroy, and Fossen (2005). The vector τ_i consists of generalized control forces and moments, and $R(\psi_i)$ is the rotation matrix between the body and Earth coordinate frame. It has the properties that $R(\psi_i)^\top R(\psi_i) = I$, $\|R(\psi_i)\| = 1$ for all ψ_i, and $(\mathrm{d}/\mathrm{d}t)R(\psi_i) = R(\psi_i)S\dot{\psi}_i$ where $S = -S^\top$ is skew-symmetric.

A group of r vessels will have r individual paths where the desired path for vessel i is given by $\eta_{di}(\theta_i) = [x_{di}(\theta_i), y_{di}(\theta_i), \psi_{di}(\theta_i)]^\top$. By careful construction, the paths are scaled appropriately such that when the vessels are in the desired formation configuration the path variables are synchronized—see Skjetne, Ihle, and Fossen (2003). The tangent vector along the path is chosen as the x-axis of the moving frame that is $T(\theta_i) = [x_{di}^{\theta_i}(\theta_i), y_{di}^{\theta_i}(\theta_i)]^\top$ where $x^{\theta_i} := \partial x/\partial\theta_i$. The desired heading can then be computed as the angle of the tangent vector in the Earth frame

$$\psi_d(\theta_i) = \arctan\left(\frac{T_y(\theta_i)}{T_x(\theta_i)}\right) = \arctan\left(\frac{y_{di}^{\theta_i}(\theta_i)}{x_{di}^{\theta_i}(\theta_i)}\right), \tag{57}$$

where $x_d(\theta_i)$ and $y_d(\theta_i)$ are three times differentiable with respect to θ_i. Then, given a path $\eta_{di}(\theta_i)$ and a speed assignment $\upsilon(t)$ as in Assumption 1 the design in Section 2 gives a path-following control law for (56)—see Ihle et al. (2004) for details.

The backstepping design for each ship model gives the static part of the control signal

$$\tau_i = -z_{1i} - K_{di}z_{2i} + D(v_i)v_i + C_i(v_i)\backslash v_i + M_i(\sigma_{1i} + \alpha_{1i}^{\theta_i}\upsilon),$$

where $K_{di} = K_{di}^\top > 0$, α_{1i} is a virtual control determined by the backstepping procedure, and $\dot{\alpha}_{1i} =: \sigma_{1i} + \alpha_{1i}^{\theta_i}\dot{\theta}$—see Skjetne et al. (2004) for details. The resulting closed-loop system is given by (9) where, for $K_{pi} = K_{pi}^\top > 0$,

$$F_i(v_i) := \begin{bmatrix} -K_{pi} - r_i S & I \\ -M_i^{-1} & -M_i^{-1}(K_{di} + D_i(v_i) + C_i(v_i)) \end{bmatrix},$$

$$g(\eta_i, \theta_i, t) := \begin{bmatrix} R(\psi_i)\eta_{di}^{\theta_i}(\theta_i) \\ \alpha_{1i}^{\theta_i}(\eta_i, \theta_i, t) \end{bmatrix}.$$

5.1. Feedback function design

The class of strictly positive real (SPR) systems includes the *filtered gradient update law* considered in Skjetne et al. (2004): we design the dynamic block $\mathscr{F}_i$ with output ω_i and dynamics

$$\dot{\omega}_i = -\lambda_i\omega_i + \gamma_i u_i, \quad \lambda_i, \gamma_i > 0. \tag{58}$$

With the storage function $V_{\omega_i} = \frac{1}{2}\omega_i^2$ we obtain $\dot{V}_{\omega_i} = -\lambda_i\omega_i^2 + \gamma_i\omega_i u_i$ and since (19)–(20) are fulfilled we invoke Theorem 1 to conclude UGAS of $(\tilde{\theta}, \omega, z) = 0$. Eq. (58) is a low-pass filter where the cut-off frequency can be designed in a trade-off fashion of measurement noise attenuation versus bandwidth, as determined by the choice of λ_i and γ_i.

The authors of Skjetne et al. (2003) discuss how thruster saturation constraints in a single vessel cause steady-state errors in the path variables synchronization. This error is eliminated by employing integral feedback from the synchronization error. In the proposed framework of Section 3 the thruster saturation can be handled with a proportional-integral-derivative (PID) control structure with limited integral and derivative effect, also known as a lead-lag controller, $\omega_i(s) = H_{pid,i}(s)u_i(s)$ given by

$$H_{pid,i}(s) = v_i\beta_i\frac{1+\mu_i s}{1+\beta_i\mu_i s}\frac{1+T_{d,i}s}{1+\alpha_i T_{d,i}s}, \tag{59}$$

where $v_i > 0$, $0 \leqslant T_{d,i} \leqslant \mu_i$, $1 \leqslant \beta_i < \infty$ and $0 < \alpha_i \leqslant 1$. Then, (59) is Hurwitz and satisfies $\mathrm{Re}[H_{pid,i}(\mathrm{j}\omega)] \geqslant v_i > 0$ for all $s = \mathrm{j}\omega$ and it follows that the PID controller structure falls into the class of input strictly passive systems and stability of the interconnection follows from Theorem 1.

5.2. Simulation: saturation in thrust

We consider a simulation where one vessel's propellers saturate and is only able to produce a surge speed less than the speed assignment. We use Design 1 in Section 3.1 and compare the synchronization error for the original control scheme in Ihle et al. (2004), i.e. $T_{d,i} = 0 = \mu_i$ in (59) while $v_i = 10$, with the PID structure with $T_{d,i} = 10$, $\mu_i = 1$, $v_i = 10$, $\alpha_i = 0.1$, and $\beta_i = 10$. The other control parameters are set as $P_i = \mathrm{diag}(0.2, 0.2, 1, 10, 10, 40)$ and $\phi_i(x) = x^3$. The desired speed is $\upsilon = 4$, and the desired path for Vessel 2 is given by $x_d(\theta_2) = \theta_2$, $y_d(\theta_2) = 1200\sin(2\pi/4000)\theta_2$, and (57). The other paths are constructed such that the vessels will move parallel when $\tilde{\theta} = 0$. The initial conditions are $\eta_1(0) = [573, 222.5, 0]^\top$, $\eta_2(0) = [0, 0, 0]^\top$, $\eta_3(0) = [320, 420, 0]^\top$, and zero initial speed. The communication topology is given by the incidence matrix

$$D(\mathscr{G}) = \begin{bmatrix} 1 & 0 \\ -1 & 1 \\ 0 & -1 \end{bmatrix}, \tag{60}$$

that is, only vehicles 1 and 2, and 2 and 3 are exchanging their path parameters. The initial synchronization errors are $\tilde{\theta}_1(0) = 500$ and $\tilde{\theta}_2(0) = -400$.

Fig. 4 shows that the formation follows the path as desired. The synchronization of $\tilde{\theta}_1$ for the two $\mathscr{F}_i$-structures are shown

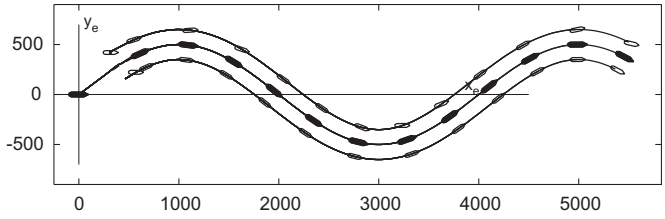

Fig. 4. Position snapshots of three tugboats where one vessel saturates. The feedback function $\mathcal{F}_i$ is as in (59).

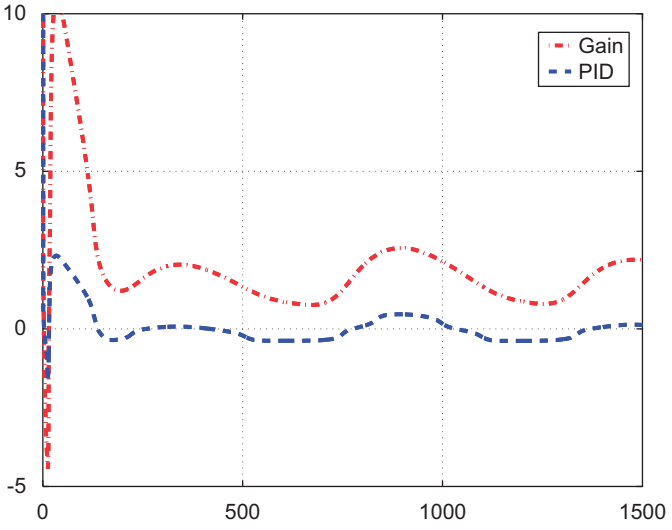

Fig. 5. Synchronization of $\tilde{\theta}_1$ when one vessel saturates. The result when $\mathcal{F}_i$ is a gain is shown in red (dashed-dot) and a PID structure for $\mathcal{F}_i$ results in the blue (dashed) plot.

in Fig. 5 and shows that the PID-structure yields a smaller error when one vessel saturates.

5.3. Simulation: time-varying communication topology

This section will study a formation with changing communication topology. Link failures and/or vessels entering and leaving the formation change the incidence matrix D and the connectivity of the formation. This section is based on results from Arcak (2007) where convergence properties for time-varying communication topology are studied for a class of agreement protocols.

The time-varying incidence matrix $D(t)$ is piecewise continuous because step changes occur when the communication topology changes. Consider the Design 2 synchronization scheme without path error feedback in Section 3.2: when the class of feedback functions $\mathcal{F}_i$ is restricted to be of the form

$$\omega_i = \gamma_i \psi_i(\theta), \tag{61}$$

where γ_i is a positive scalar, it is shown in Arcak (2007) that, if the second smallest eigenvalue for the graph Laplacian matrix $D(t)D(t)^\top$ satisfies

$$\lambda_2\{D(t)D(t)^\top\} \geqslant \sigma > 0 \quad \forall t \geqslant 0 \tag{62}$$

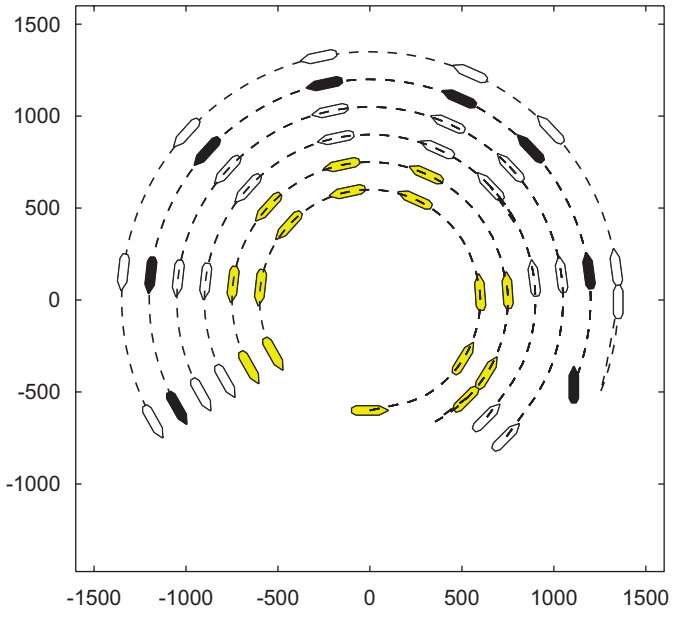

Fig. 6. Eight position snapshots of formation. The vessels are in the beginning synchronized into two groups (second snapshot). After t_{change} all vessels are synchronized and move in parallel. Vessel 2 is shown in black.

for some constant time-independent $\sigma > 0$, the path parameters $\tilde{\theta}_i$ reach an agreement. It is a standard result in algebraic graph theory that the graph is connected if and only if the Laplacian's second smallest eigenvalue is strictly positive. Thus, for the design considered in Section 3.2 with feedback functions as in (61), the vessels synchronize if the graph remains connected for all $t \geqslant 0$.

Arcak (2007) relaxes this connectivity assumption with a persistency of excitation property. The graph can then loose connectivity pointwise in time as long as it is established in an integral sense. To illustrate stability properties we consider a formation of six vessels that are initially grouped as two formations. After some time the two groups merge into one, and at the same time one vessel experience communication problems and is only able to communicate 10% of the time.

Vessel 2 (shown in black in Fig. 6) shall follow a circle-shaped path given by

$$\eta_{d2}(\theta_2) = \begin{bmatrix} x_d(\theta_2) \\ y_d(\theta_2) \\ \psi_d(\theta_2) \end{bmatrix} = \begin{bmatrix} r\cos\left(\dfrac{\theta_2}{r}\right) \\ r\sin\left(\dfrac{\theta_2}{r}\right) \\ \arctan\left(\dfrac{x_d^{\theta_2}(\theta_2)}{y_d^{\theta_2}(\theta_2)}\right) \end{bmatrix},$$

where $r = 1200$ m is the radius. The other paths are scaled such that equal speed assignments imply that, after synchronization of all path parameters has occurred, the vessels will move along their respective paths parallel to each other. The initial values for the vessels are $\eta_1 = [1350, 0, \pi/2]^\top$, $\eta_2 = [1109, -459, \pi/2]^\top$, $\eta_3 = [742, -742, \pi/4]^\top$, $\eta_4 = [636, -363, \pi/4]^\top$, $\eta_5 = [530, -530, \pi/4]^\top$, and $\eta_6 = [0, -600, 0]^\top$ with zero initial

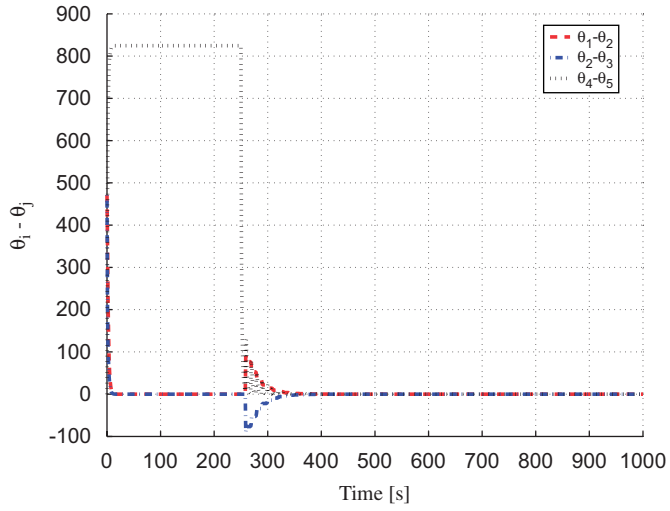

Fig. 7. Synchronization of path parameters with time-varying communication topology using Design 2.

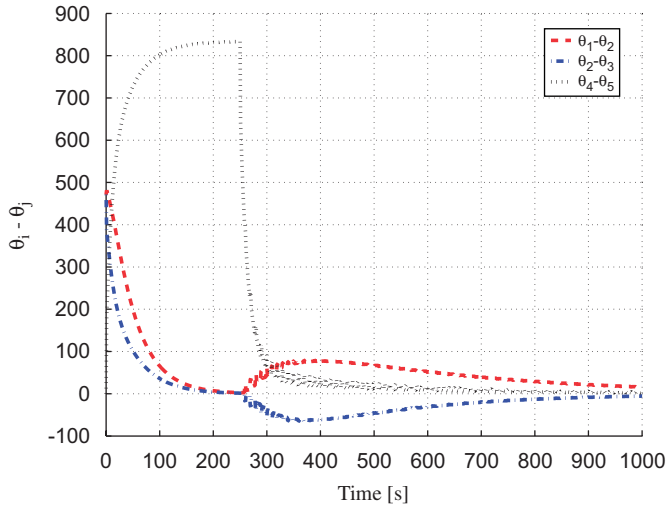

Fig. 8. Synchronization of path parameters with time-varying communication topology using Design 1.

speeds. The initial synchronization errors, given by $\tilde{\theta} = D^\top \theta$, are $\tilde{\theta} = [471, 471, 471, 0, 942]^\top$. The synchronization function is $\psi(x) = 0.1x$ and $\gamma_i = 5$.

For $t < t_{\text{change}} = 250\,\text{s}$ vessels 1, 3 and 4 communicate with vessel 2 while vessel 4 communicates with vessel 5. Thus, there are initially two decoupled formations as seen in Fig. 6 where the two innermost vessels, that is vessels 5 and 6, and the other group synchronize separately. This is also seen in Fig. 7 which shows the time-response of $\tilde{\theta}_1$, $\tilde{\theta}_2$, $\tilde{\theta}_4$. Before t_{change} we see that e.g. $\tilde{\theta}_1$ tend to zero while $\tilde{\theta}_4 = \theta_4 - \theta_5$ reaches a nonzero value even though the initial condition is zero. When $t = t_{\text{change}}$ the entire formation is connected, but vessel 2 is now only able to send and receive the path parameters 10% of the time. The time-response of the path parameters in Fig. 7 shows that the vessel synchronize and stay that way throughout the simulation.

To compare performance the same scenario has been simulated in the framework of Design 1 where path error information is used in the synchronization (11). Fig. 8 shows that all $\tilde{\theta}_i$ tend to zero in the presence of link failures which cause some oscillations in the path parameters as the vessels synchronize. Both designs synchronize the vessels in the formation, but the plots in Figs. 7 and 8 show that Design 2 is less sensitive to communication constraints as the vessels synchronize faster and with less oscillations than with Design 1.

Simulations with the sampled-data design, which are omitted due to space limitations, yield similar trajectories to the continuous-time designs for sufficiently small sampling periods.

6. Discussion and conclusions

This paper has used passivity properties to design a formation control scheme where path-following systems are synchronized using a bidirectional communication structure. The first design used feedback from both the path error and the synchronization error in the update law for the path parameter, while the second only employed information about the synchronization error. The path error feedback in Design 1 emphasizes convergence to the path while the synchronization error feedback achieves the desired formation. This scheme thus enables the designer to prioritize path convergence or synchronization by choosing the relative gains of the two feedback terms. Furthermore, the system can employ its own path error information to handle situations where a trajectory tracking scheme has limitations (Aguiar et al., 2005)—one example is control saturation where an infeasible speed assignment cause instabilities (Fossen, 2002, Chapter 10). However, our analysis for Design 1 is only valid for time-invariant graph structures.

Design 2 inherits the properties of the coordination scheme in Arcak (2007) where a time-varying formation configuration is tolerated. In addition, since the incidence matrix D does not have to be pointwise connected for all times, communication dropouts are allowed, and similarly, vehicles can enter or leave the formation. Simulations show that synchronization occurs faster with Design 2 and is less sensitive to communication constraints since synchronization occurs faster when only path parameters are employed in the design. However, by disregarding the path error information the designer has less control on the convergence to the path.

A sampled-data approach to synchronization, where the synchronization scheme is updated in discrete-time and the path-following systems in continuous time, is considered. The main motivation is that communication of path variables will likely occur over a digital network and a discrete-time system is more natural to model communication of path parameters.

Acknowledgments

The authors would like to thank Emrah Biyik for his help on Section 4.

References

Aguiar, A. P., Hespanha, J. P., & Kokotović, P. V. (2005). Path-following for non-minimum phase systems removes performance limitations. *IEEE Transactions on Automatic Control*, *50*(2), 234–239.

Al-Hiddabi, S. A., & McClamroch, N. H. (2002). Tracking and maneuver regulation control for nonlinear nonminimum phase systems: Application to flight control. *IEEE Transactions on Control Systems Technology*, *10*(6), 780–792.

Arcak, M. (2007). Passivity as a design tool for group coordination. *IEEE Transactions on Automatic Control*, in press.

Biyik, E., & Arcak, M. (2006). Passivity-based agreement protocols: Continuous-time and sampled-data designs. In K. Y. Pettersen, T. Gravdahl, & H. Nijmeijer (Eds.), *Group coordination and cooperative control*, *Lecture notes in control and information sciences* (Vol. 336, pp. 21–33). Berlin Heidelberg: Springer.

Do, K. D., Jiang, Z. P. & Pan, J. (2002). Robust adaptive path-following of underactuated ships. In *Proceedings of the 41st IEEE conference on decision and control* (pp. 3243–3248). Las Vegas, NV, USA.

Encarnação, P., & Pascoal, A. (2001). Combined trajectory tracking and path-following: An application to the coordinated control of autonomous marine craft. In *Proceedings of the 40th IEEE conference on decision and control* (pp. 964–969). Orlando, FL, USA.

Fossen, T. I. (2002). *Marine control systems: Guidance, navigation and control of ships, rigs and underwater vehicles*. Trondheim, Norway: Marine Cybernetics, ⟨http://www.marinecybernetics.com⟩.

Godsil, C. D., & Royle, G. F. (2001). *Algebraic Graph Theory*, *Graduate texts in mathematics* (Vol. 207). New York: Springer.

Hauser, J., & Hindman, R. (1995). Maneuver regulation from trajectory tracking: Feedback linearizable systems. In *Proceedings of the IFAC symposium on nonlinear control systems design* (pp. 595–600). Lake Tahoe, CA, USA.

Ihle, I.-A. F., Jouffroy, J., & Fossen, T. I. (2005). Formation control of marine surface craft using Lagrange multipliers. In *Proceedings of the 44th IEEE conference on decision and control and 5th European control conference* (pp. 752–758). Seville, Spain.

Ihle, I.-A. F., Skjetne, R., & Fossen, T. I. (2004). Nonlinear formation control of marine craft with experimental results. In *Proceedings of the 43rd IEEE conference on decision and control* (pp. 680–685). Atlantis, Paradise Island, The Bahamas.

Khalil, H. K. (2002). *Nonlinear systems*. (3rd ed.), New York: Prentice-Hall.

Kumar, V., Leonard, N., & Morse, A. S. (Eds.) (2005). *Cooperative control*, *Lecture notes in control and information sciences* (Vol. 309). Berlin, Heidelberg: Springer.

Laila, D. S., Nešić, D., & Teel, A. R. (2002). Open and closed loop dissipation inequalities under sampling and controller emulation. *European Journal of Control*, *8*(2), 109–125.

Loría, A., Panteley, E., Popović, D., & Teel, A. R. (2005). A nested matrosov theorem and persistency of excitation for uniform convergence in stable nonautonomous systems. *IEEE Transactions on Automatic Control*, *50*(2), 183–198.

Ren, W., Beard, R. W., & Atkins, E. M. (2005). A survey of consensus problems in multi-agent coordination. In *Proceedings of the American control conference* (pp. 1859–1864). Portland, OR, USA.

Samson, C. (1992). Path following and time-varying feedback stabilization of a wheeled mobile robot. In *Proceedings of the ICARCV'92'*, Singapore.

Sepulchre, R., Janković, M., & Kokotović, P. (1997). *Constructive nonlinear control*. New York: Springer.

Skjetne, R., Fossen, T. I., & Kokotović, P. V. (2004). Robust output maneuvering for a class of nonlinear systems. *Automatica*, *40*(3), 373–383.

Skjetne, R., Ihle, I.-A. F., & Fossen, T. I. (2003). Formation control by synchronizing multiple maneuvering systems. In *Proceedings of the 6th IFAC conference on maneuvering and control of marine crafts* (pp. 280–285). Girona, Spain.

Skjetne, R., Teel, A. R., & Kokotović, P. V. (2002). Nonlinear maneuvering with gradient optimization. In *Proceedings of the 41st IEEE conference on decision and control* (pp. 3926–3931). Las Vegas, NV, USA.

Sontag, E., & Teel, A. (1995). Changing supply functions in input/state stable systems. *IEEE Transactions on Automatic Control*, *40*, 1476–1478.

Sontag, E. D. (1989). Smooth stabilization implies coprime factorization. *IEEE Transactions on Automatic Control*, *34*(4), 435–443.